Electronic Supplementary Information

A difluorobenzothiadiazole-based conjugated polymer with alkylthiophene as the side chains for efficient, additive-free and thick-film polymer solar cells

Mu He, § [a, d] Miaomiao Li, § [b, c] Xin Dong,[a, d] Hongkun Tian,*[a] Hui Tong,*[a] Jun Liu,[a] Zhiyuan Xie,[a] Yanhou Geng*[a, b, c] and Fosong Wang[a]

§ M.M. Li and Y.T. Liu contributed equally to this work.

[a] State Key Laboratory of Polymer Physics and Chemistry, Changchun Institute of Applied Chemistry, Chinese Academy of Sciences, Changchun, 130022, P. R. China.

*E-mail: yanhou.geng@tju.edu.cn; hktian@ciac.ac.cn; chemtonghui@ciac.ac.cn

[b] School of Materials Science and Engineering and Tianjin Key Laboratory of Molecular Optoelectronic Science, Tianjin University, Tianjin 300072, P. R. China.

[c] Collaborative Innovation Center of Chemical Science and Engineering (Tianjin), Tianjin University, Tianjin 300072, P. R. China.

[d] University of Chinese Academy of Sciences, Beijing, 100049, P. R. China.

Instruments

^{1}H NMR and ^{13}C NMR solution spectra were recorded on a Bruker AV (400 MHz for ^{1}H, 100 MHz for ^{13}C and 376 MHz for ^{19}F) spectrometer with chloroform-d (CDCl$_3$, tetramethylsilane (TMS) as an internal standard), methylene chloride-d$_2$ (CD$_2$Cl$_2$, TMS as an internal standard) or 1,1,2,2-tetrachlororoethane-d$_2$ (C$_2$Cl$_4$D$_2$) as solvent. Matrix-assisted laser desorption ionization time-of-flight (MALDI-TOF) mass spectra were measured on a Bruker/AutoflexIII Smartbean MALDI mass spectrometer with 2-[(2E)-3-(4-t-buthylphenyl)-2-methylprop-2-enylidene]malononitrile (DCTB) as the matrix in a reflection mode. The molecular weight of polymers was determined via high-temperature gel permeation chromatography (GPC) on a PL-GPC 220 system at 150 ^{o}C, with 1,2,4-trichlorobenzene as eluent and monodisperse polystyrene as standard. UV-Vis absorption spectra were recorded on a Shimadzu UV3600 UV-vis-NIR spectrometer. The optical band gap was calculated according to the absorption onset of spectra (E^{opt}_g = 1240/λ_{onset} eV). Cyclic voltammetry (CV) measurements were carried out on a CHI660a electrochemical workstation at a scan rate of 100 mV s^{-1}. The CV cell consisted of glassy carbon electrode (diameter of 1 cm) as working electrode, saturated calomel electrode as reference electrode and platinum wire as counter electrode. NBu$_4$PF$_6$ (0.1M) in anhydrous acetonitrile was used as electrolyte. To extract the energy levels of polymer films, the potential was calibrated against ferrocene/ferrocenium (Fc/Fc$^+$). HOMO and LUMO energy levels were calculated by the equations: HOMO = $-(4.80 + E^{ox}_{onset})$ eV and LUMO = $-(4.80 + E^{re}_{onset})$ eV, in which E^{ox}_{onset} and E^{re}_{onset} are oxidation and reduction onsets versus the half potential of

Fc/Fc$^+$, respectively. TGA was performed at a heating rate of 10 °C min^{-1} under nitrogen flow on a PerkinElmer TGA7. DSC was carried out on a PerkinElmer DSC 7 with a heating/cooling rate of ±10 °C min^{-1} under nitrogen flow. Two-dimensional grazing-incidence wide angle X-ray scattering (2D-GIWAXS) was measured at Shanghai Synchrotron Radiation Facility (SSRF) on beam line BL14B1 (λ = 0.0689 nm) with a MarCCD area detector at incidence angle of 0.16°. Atomic force microscopy (AFM) measurements were carried out in tapping mode on a SPA400HV instrument with a SPI 3800 controller (Seiko Instruments). Transmission electron microscopy (TEM) images were recorded on a JEM-1011 transmission electron microscope with accelerating voltage of 100 KV and camera length of 160 cm.

Fabrication and characterization of PSC devices

PSC devices with a device configuration of ITO/ PEDOT:PSS (~40 nm)/polymer:PC$_{71}$BM /PFN (~5 nm)/Al (100 nm) were fabricated. Pre-patterned indium tin oxide (ITO) coated glass substrates were cleaned sequentially with detergent, deionized water, acetone and isopropanol in ultra-sonication, followed by drying at 120 °C for 30 min and ultraviolet/ozone treatment for 25 min. PEDOT:PSS layer (Baytron P Al 4083) with thickness of ~40 nm was prepared via spin-coating on the ITO-glass substrates at 5000 r.p.m. for 40 s. After baking at 120 °C for 30 min, the substrates were transferred into glovebox under N$_2$ atmosphere. Polymer:PC$_{71}$BM solutions were prepared in *o*-DCB as solvent (polymer concentration: 11 mg/mL for both **P-2T** and **P-TT**) and were stirred on a hotplate (~ 115 °C) for at least 4 h in N$_2$

glovebox. Before spin coating, both the solutions and the substrates were pre-heated on a hotplate (at 90 °C for **P-2T** and 110 °C for **P-TT**). Active layers were spin coated from the warm solutions on the pre-heated substrates in N_2 glovebox. After the active layers were dried under low vacuum (< 10 Pa) for 30 min, PFN layer with thickness of ~ 5 nm was spin coated from a MeOH solution (concentration: 0.25 mg/mL) on active layer at 3000 r.p.m. for 30 s. Finally, Al layer with thickness of 100 nm was deposited by thermal evaporation at the pressure of ~ 2×10^{-4} Pa in a vacuum chamber. The active area of devices is 8 mm². Keithley 2400 source meter was used to measure *J-V* curves under 100 mW cm⁻² AM 1.5G simulated solar light illumination provided by a XES-40S2-CE Class Solar Simulator (Japan, SAN-EI Electric Co., Ltd.) in a glove box. EQE curves were detected on a QE-R3011IPCE measurement system (Enli Technology Co. Ltd).

SCLC measurement

The charge carrier mobilities of blend films were measured using the SCLC method. Hole-only and electron-only devices were fabricated with configuration of ITO/PEDOT:PSS (40 nm)/active layer (300 nm)/MoO₃ (10 nm)/Al (100 nm) and ITO/PEIE (10 nm)/active layer (300 nm)/PFN (5 nm)/Al (100 nm) respectively. The devices were measured using Keithley 2400 source meter in the dark and the charge carrier mobilities were calculated by fitting the results using a space-charge limited function[1]:

$$J = \frac{9}{8}\varepsilon_0\varepsilon_r\mu\frac{V^2}{L^3}exp(0.89\beta\frac{\sqrt{V}}{\sqrt{L}})$$

Where J is the dark current density, ε_0 is the permittivity of free space, ε_0 is the dielectric constant and is assumed to be 3 in our analysis, μ is the charge carrier mobility, V is the voltage drop across the device and L is the thickness of the blend layer.
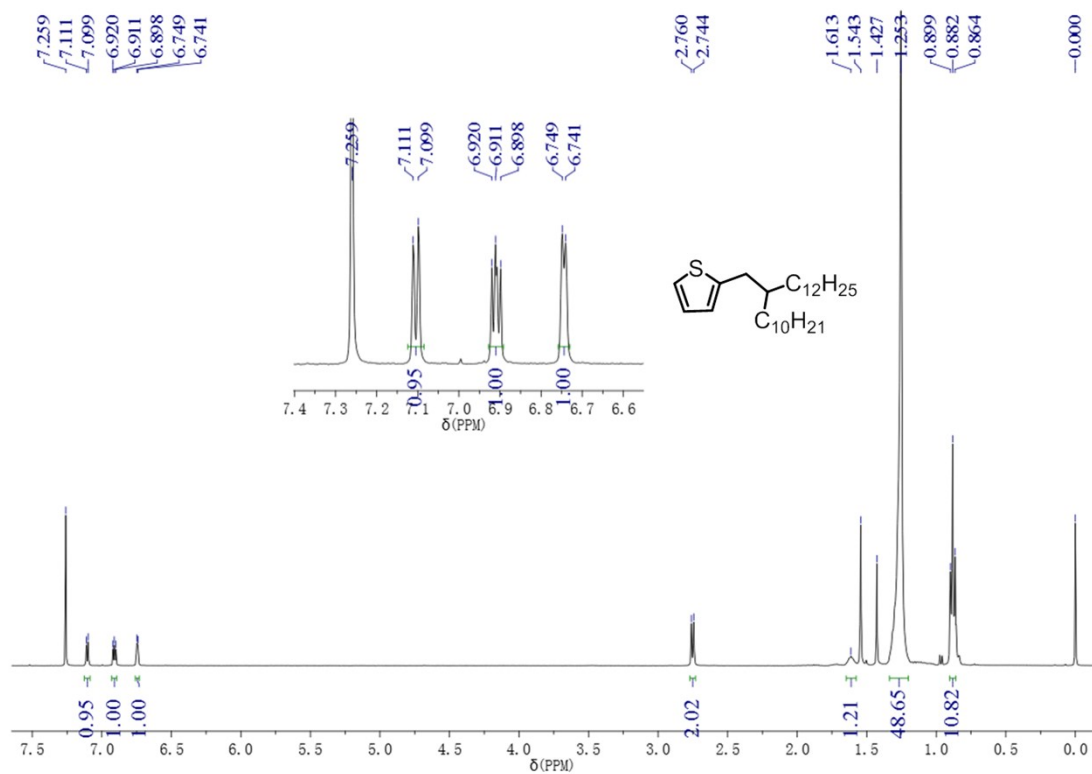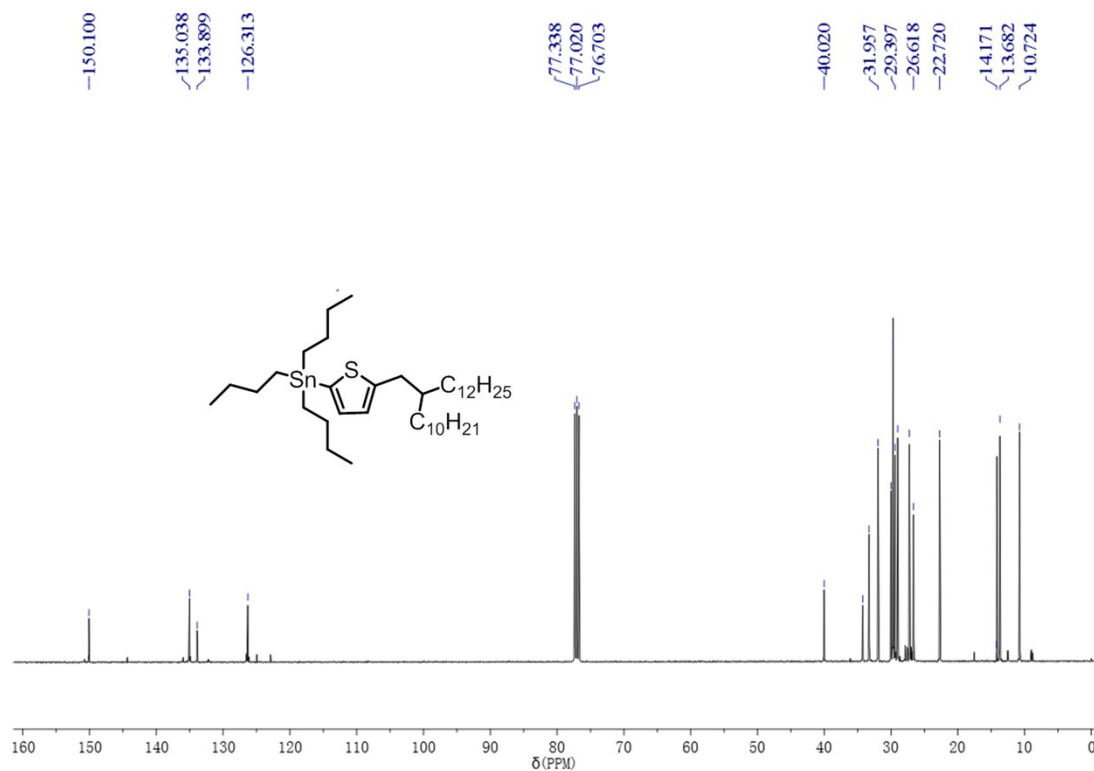
Fig. S1 ^{1}H NMR spectra of 2-(2-decyltetradecyl)thiophene (**2**).
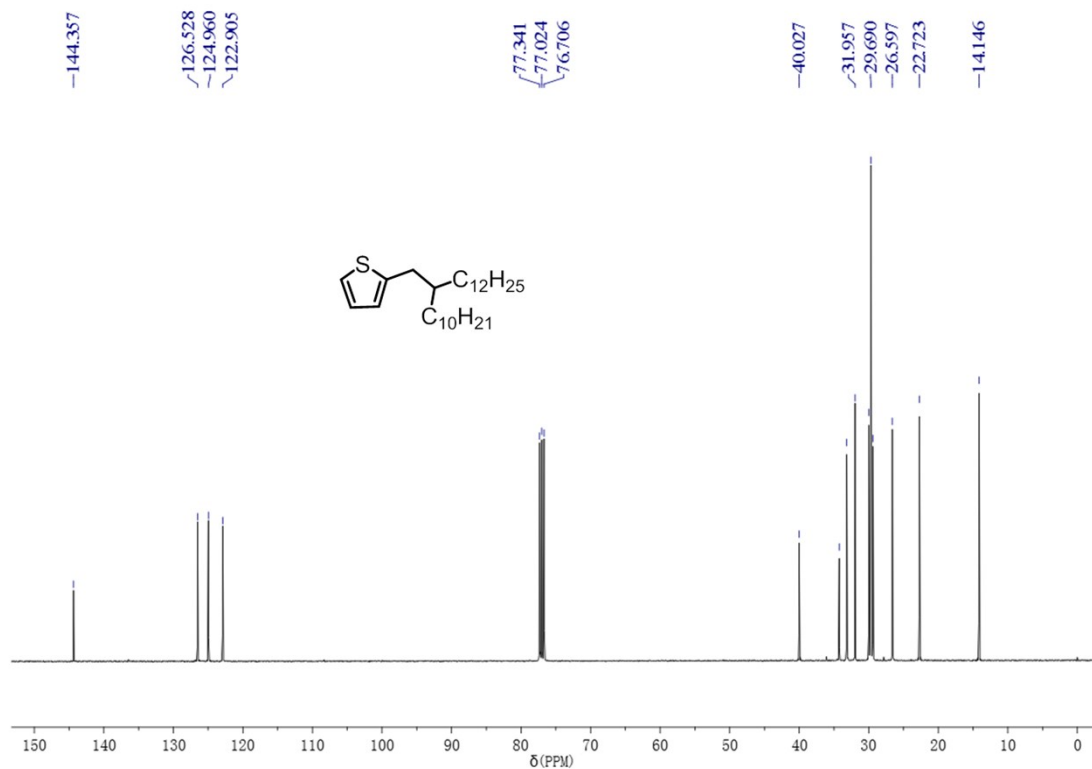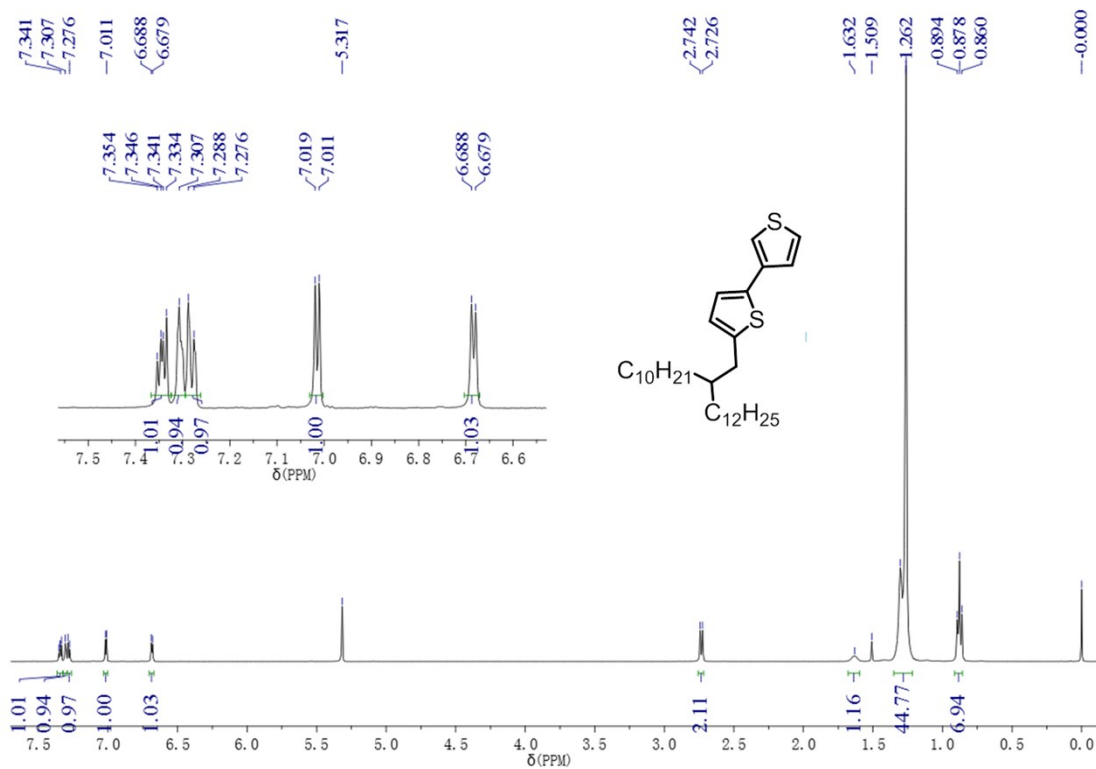

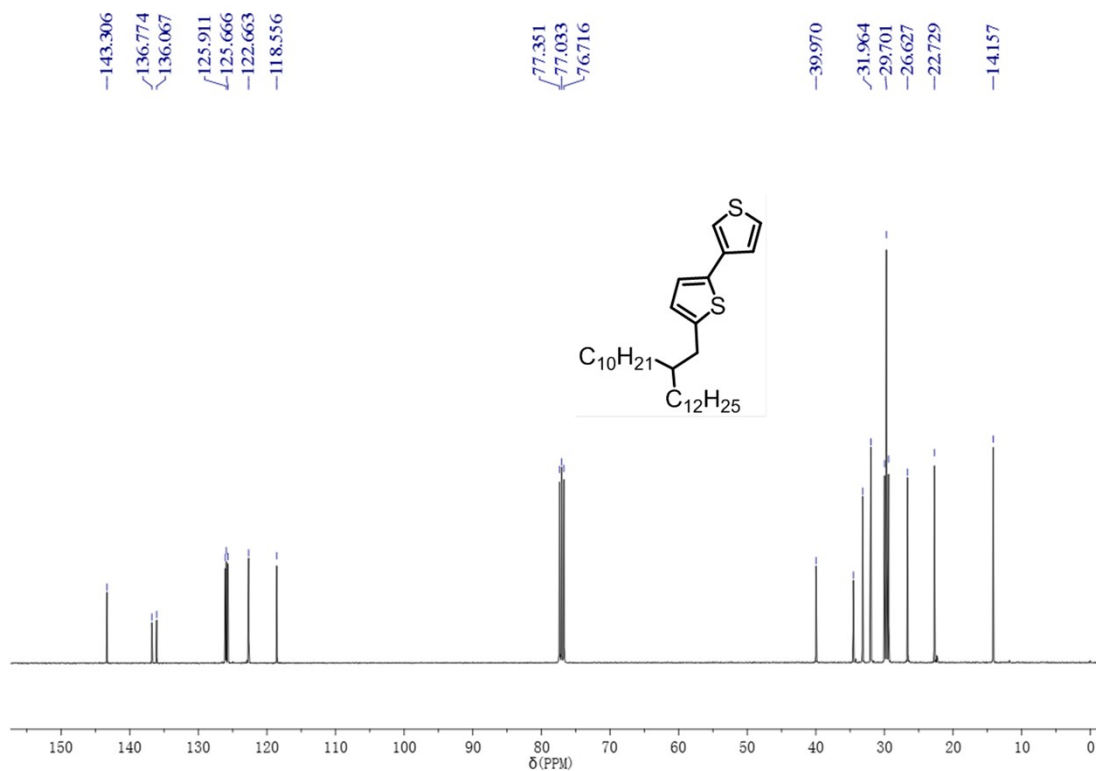**Fig. S2** ^{13}C NMR spectra of 2-(2-decyltetradecyl)thiophene (**2**).
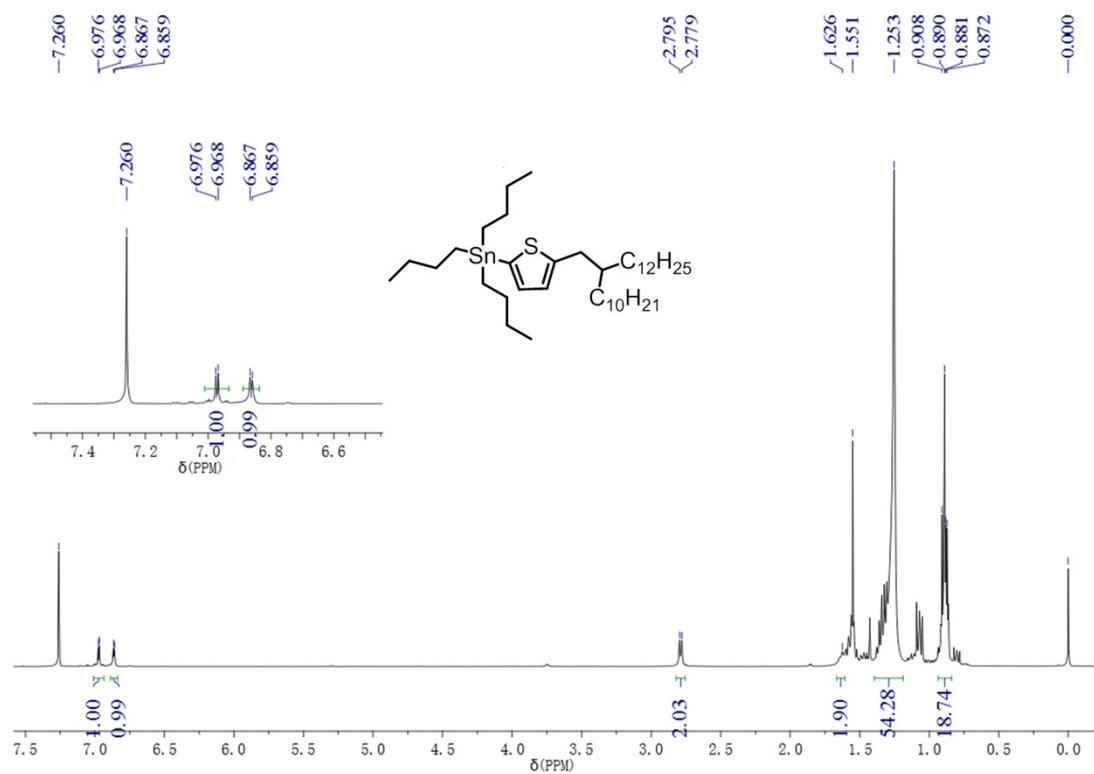
Fig. S3 ¹H NMR spectra of tributyl(5-(2-decyltetradecyl)thiophen-2-yl)stannane (**3**).

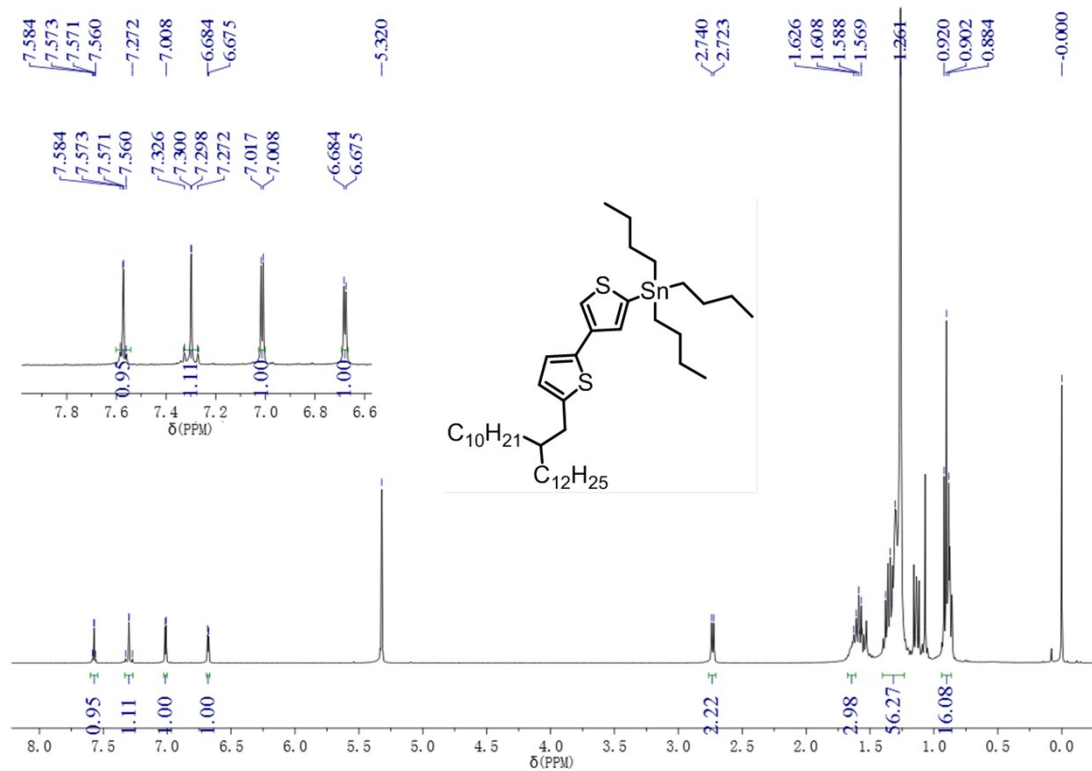**Fig. S4** ¹³C NMR spectra of tributyl(5-(2-decyltetradecyl)thiophen-2-yl)stannane (**3**).

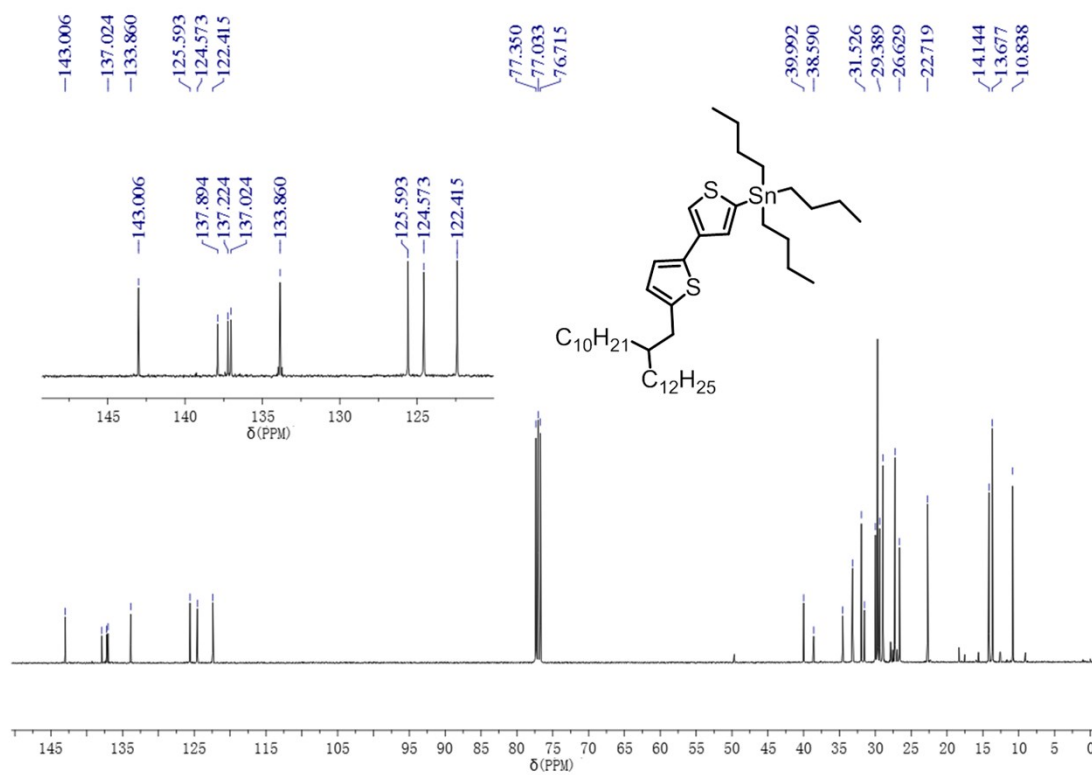**Fig. S5** ^{1}H NMR spectra of 5-(2-decyltetradecyl)-2,3'-bithiophene (**4**).

Fig. S6 ^{13}C NMR spectra of 5-(2-decyltetradecyl)-2,3'-bithiophene (**4**).
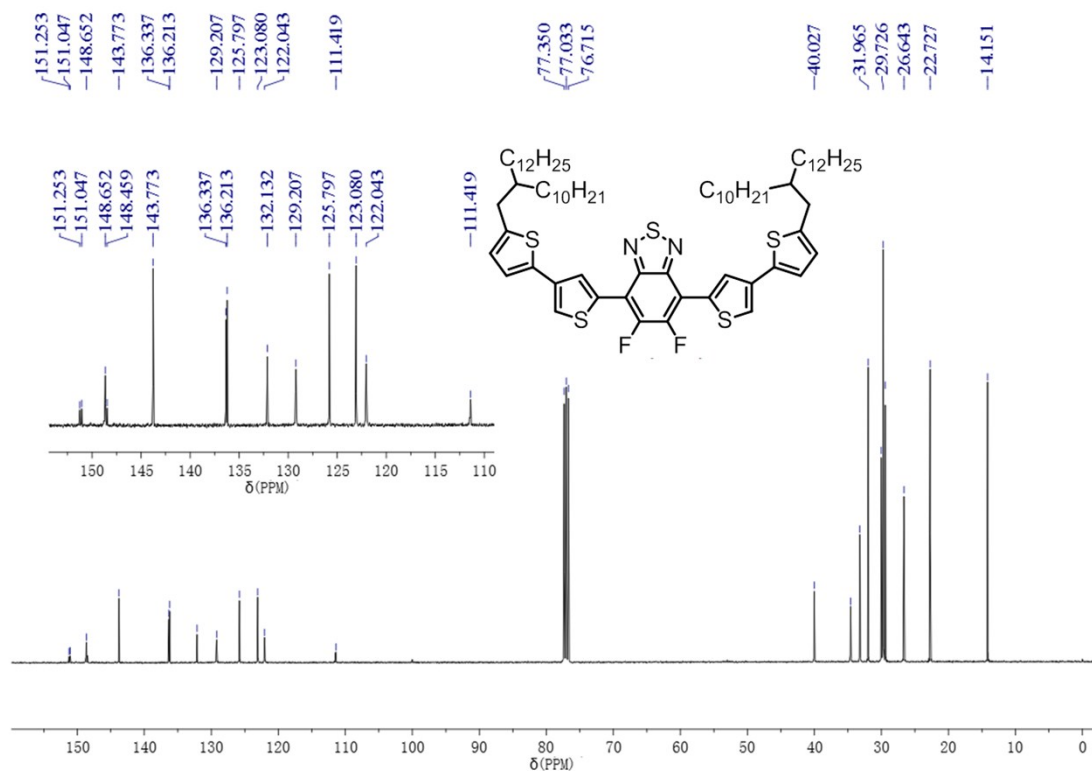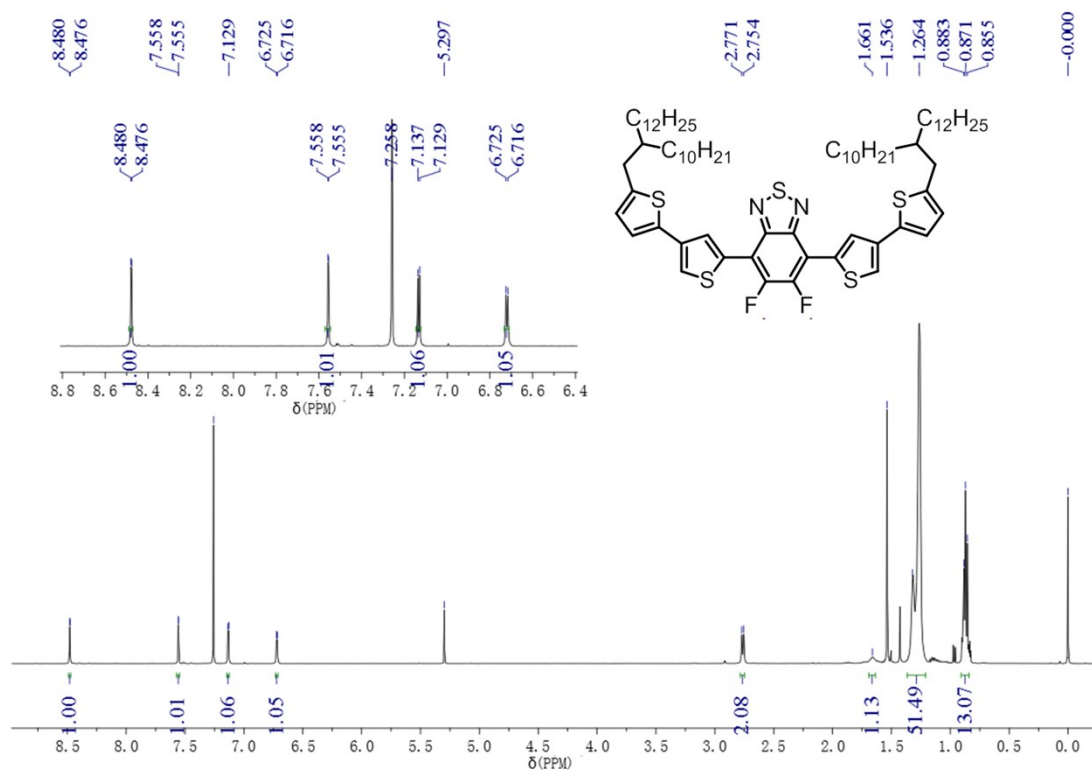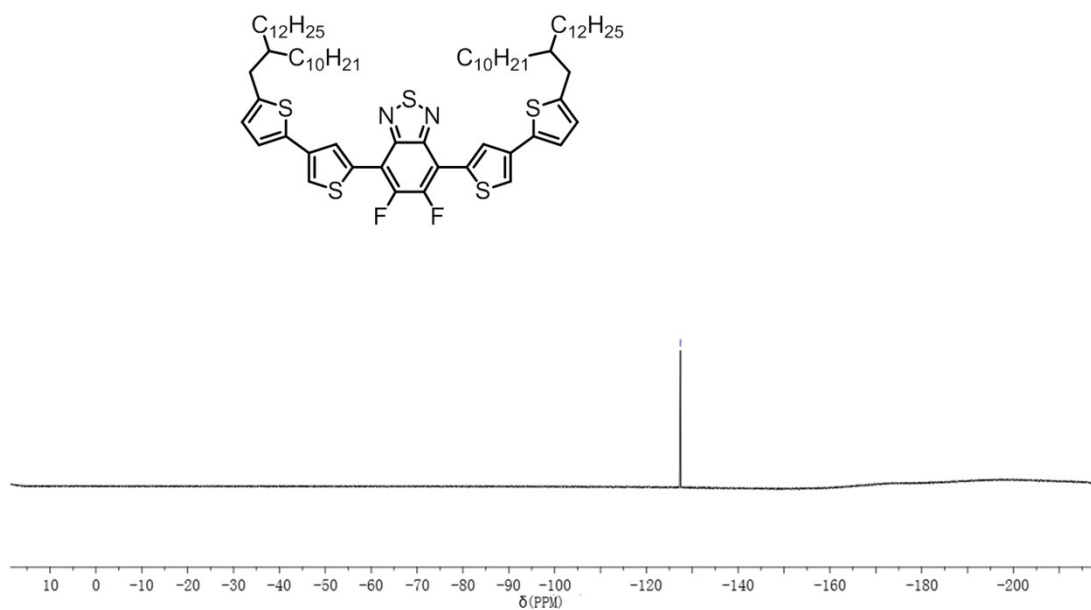
Fig. S7 ^{1}H NMR spectra of (5-(2-decyltetradecyl)-[2,3'-bithiophen]-5'-yl)trimethylstannane (**5**).
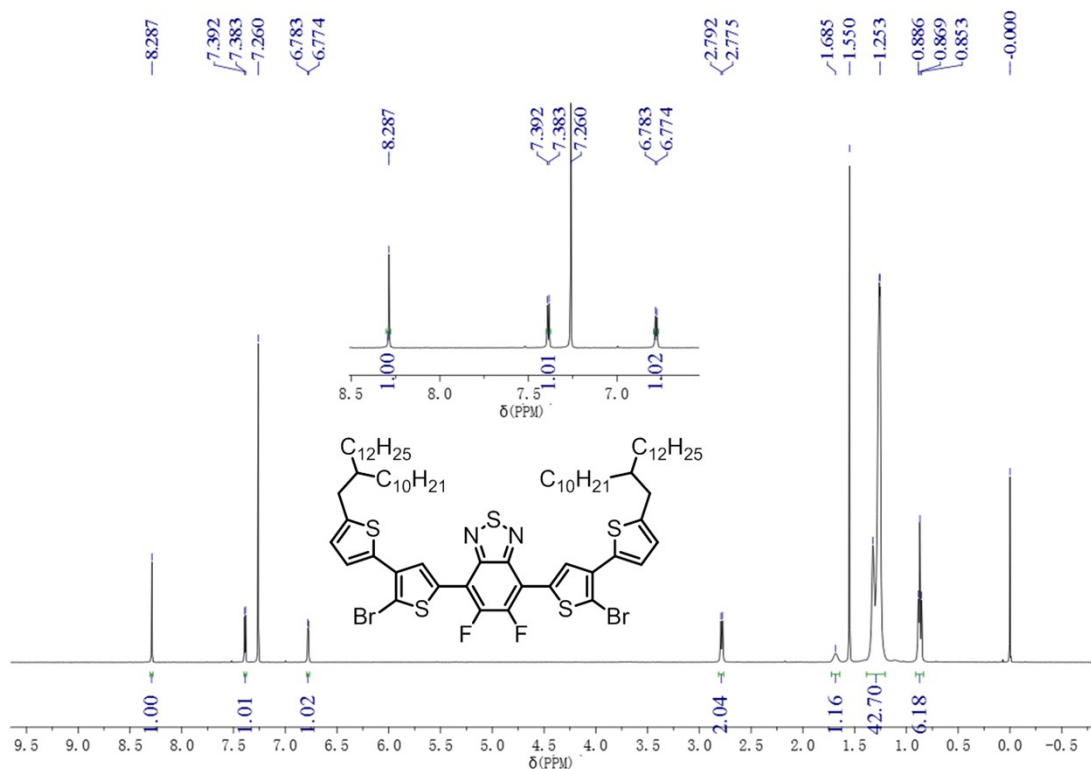

Fig. S8 ^{13}C NMR spectra of (5-(2-decyltetradecyl)-[2,3'-bithiophen]-5'-yl)trimethylstannane (**5**).

Fig. S9 ^{1}H NMR spectra of 4,7-bis(5-(2-decyltetradecyl)-[2,3'-bithiophen]-5'-yl)-5,6-difluorobenzo[c][1,2,5]thiadiazole (**6**).

Fig. S10 ^{13}C NMR spectra of 4,7-bis(5-(2-decyltetradecyl)-[2,3'-bithiophen]-5'-yl)-5,6-difluorobenzo[c][1,2,5]thiadiazole (**6**).
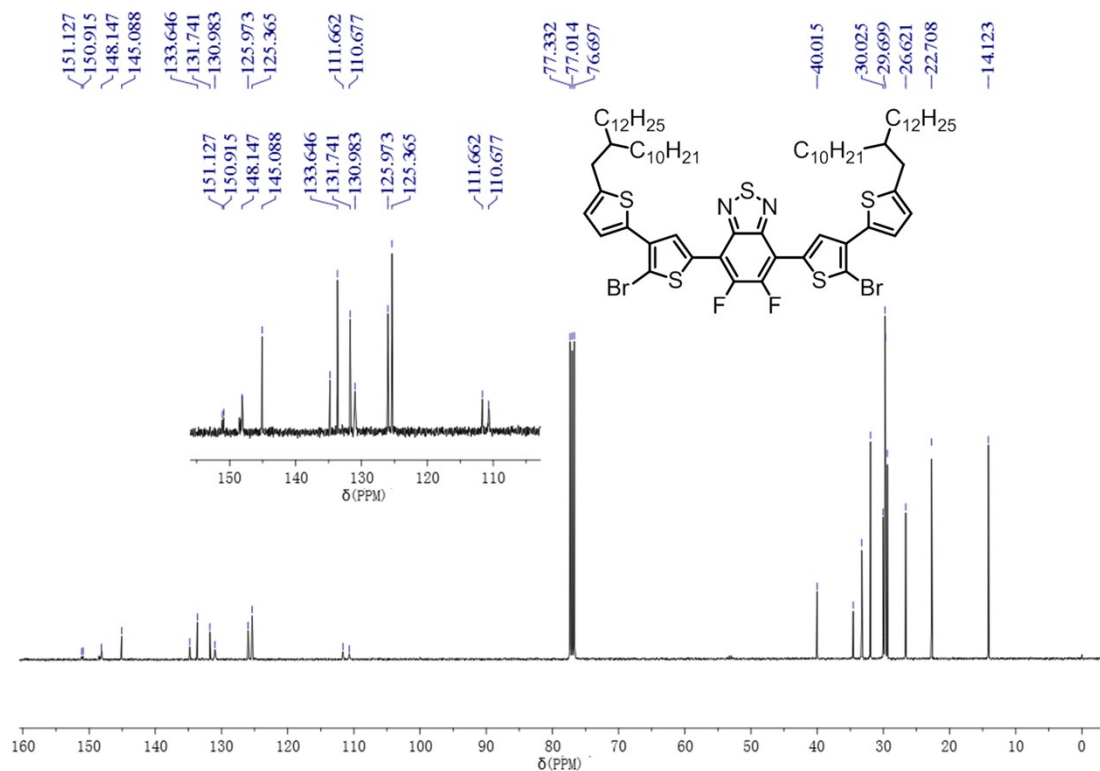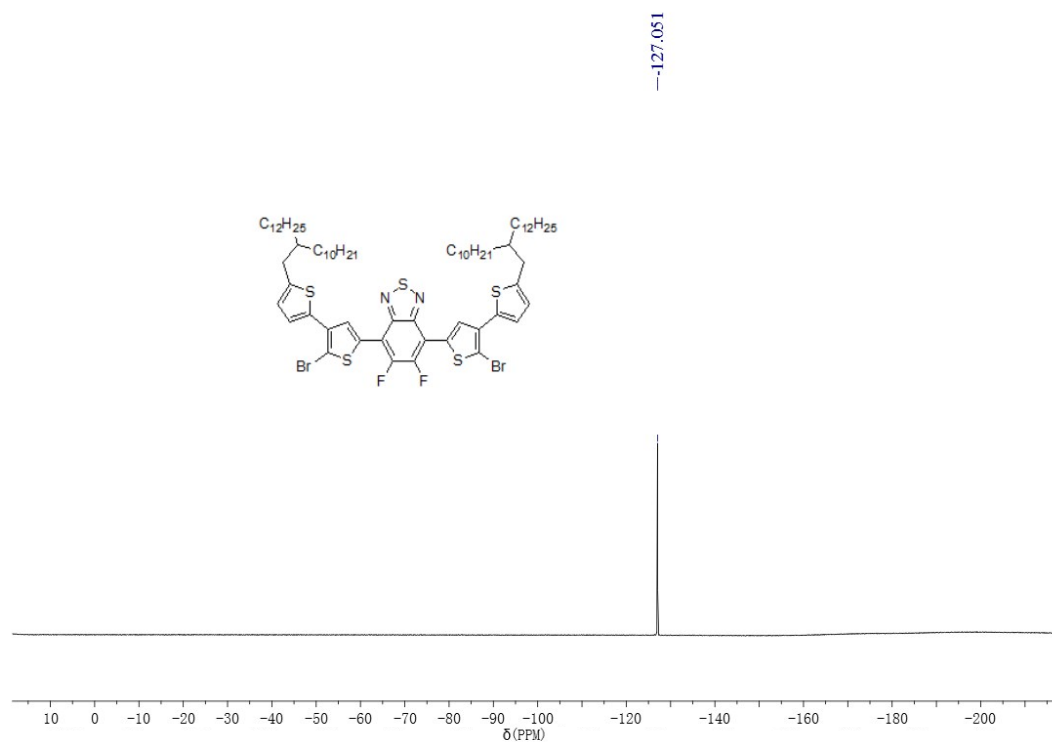
−127.413

Fig. S11 ^{19}F NMR spectra of 4,7-bis(5-(2-decyltetradecyl)-[2,3'-bithiophen]-5'-yl)-5,6-difluorobenzo[c][1,2,5]thiadiazole (**6**).

Fig. S12 ^{1}H NMR spectra of 4,7-bis(2'-bromo-5-(2-decyltetradecyl)-[2,3'-bithiophen]-5'-yl)-5,6-difluorobenzo[c][1,2,5]thiadiazole (**7**).
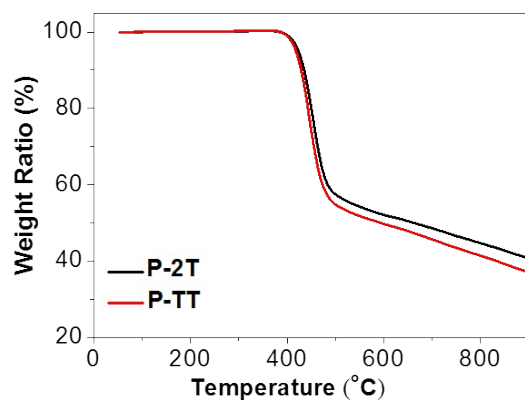
Fig. S13 ^{13}C NMR spectra of 4,7-bis(2'-bromo-5-(2-decyltetradecyl)-[2,3'-bithiophen]-5'-yl)-5,6-difluorobenzo[c][1,2,5]thiadiazole (**7**).

Fig. S14 ^{19}F NMR spectra of 4,7-bis(2'-bromo-5-(2-decyltetradecyl)-[2,3'-bithiophen]-5'-yl)-5,6-difluorobenzo[c][1,2,5]thiadiazole (**7**).

Fig. S15 ^{1}H NMR spectra of **P-2T**.

Fig. S16 ^{1}H NMR spectra of **P-TT**.

Fig. S17 TGA curves of the polymers in nitrogen with a heating rate of 10 °C/min.
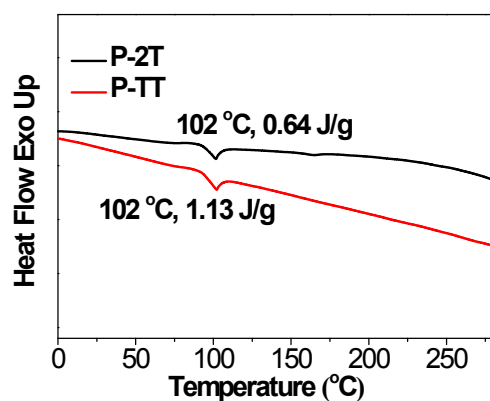
Fig. S18 DSC curves of the polymers: in nitrogen with a heating/cooling rate of 10 °C/min.

Fig. S19 Thin film cyclic voltammograms (CV) of the polymers.

Fig. S20 *J-V* curves of **P-2T** based PSC devices at different a) donor-acceptor ratio and b**)** active layer thickness.
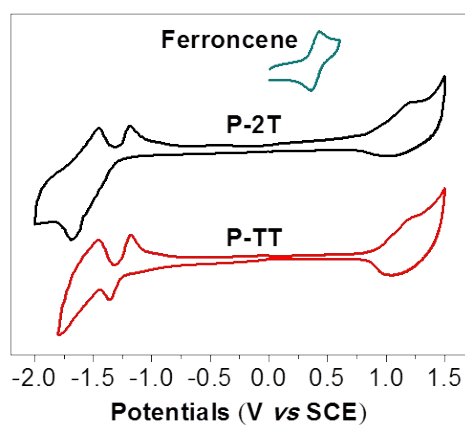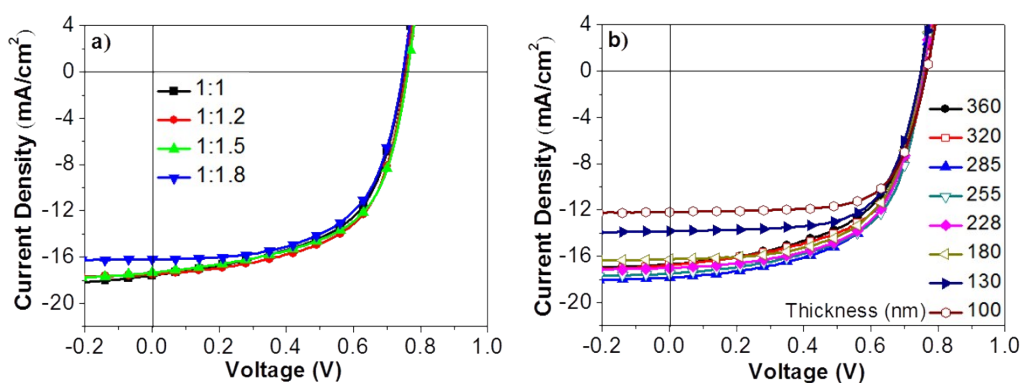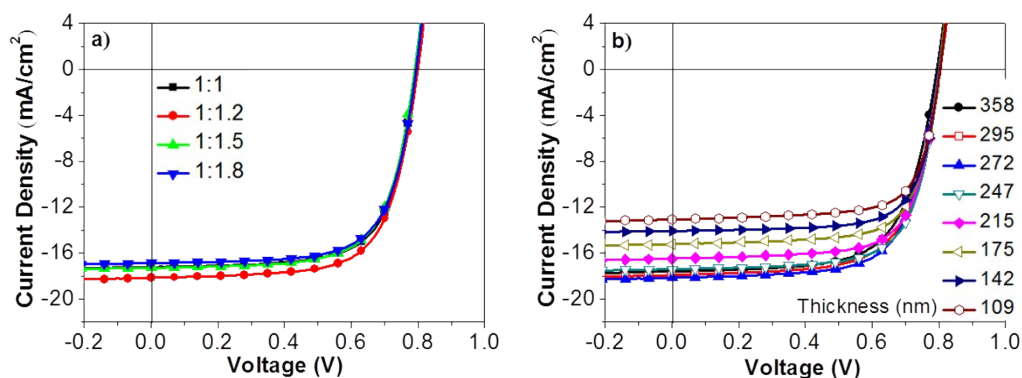
Table S1 The detailed photovoltaic performances of the solar cells based on **P-2T**:$PC_{71}BM$ with different D:A ratio (wt:wt) and active layer thickness. The solvent was *o*-DCB.

D:A ratio	Thickness (nm)	J_{sc} (mA/cm²)	V_{oc} (V)	FF	PCE_{max} (PCE_{ave}) [a] (%)
1:1	288	17.57	0.75	57.3%	7.55 (7.39)
1:1.5	271	17.34	0.76	58.9%	7.76 (7.47)
1:1.8	242	16.20	0.75	60.2%	7.31 (7.16)
	360	16.69	0.75	56.7%	7.10 (6.94)
	320	16.78	0.76	58.0%	7.40 (7.22)
	285	17.83	0.76	58.1%	7.87 (7.61)
1:1.2	255	17.48	0.76	59.5%	7.91 (7.69)
	228	17.01	0.75	61.0%	7.78 (7.54)
	180	16.26	0.76	61.4%	7.48 (7.14)
	130	13.82	0.75	66.3%	6.88 (6.75)
	100	12.18	0.77	68.8%	6.45 (6.30)

[a] The values in parentheses stand for the average PCEs from over 15 devices.

Fig. S21 *J-V* curves of **P-TT** based PSC devices at different a) donor-acceptor ratio and b**)** active layer thickness.

Table S2 The detailed photovoltaic performances of the solar cells based on **P-TT**:$PC_{71}BM$ with different D:A ratio (wt:wt) and active layer thickness. The solvent was *o*-DCB.

D:A ratio	Thickness (nm)	J_{sc} (mA/cm^2)	V_{oc} (V)	FF	PCE$_{max}$ (PCE$_{ave}$) [a] (%)
1:1	260	17.20	0.79	69.7%	9.47 (9.11)
1:1.5	254	17.11	0.80	69.9%	9.57 (9.33)
1:1.8	264	16.77	0.79	69.6%	9.22 (8.88)
1:1.2	358	17.60	0.79	66.9%	9.30 (8.90)
	295	17.91	0.80	67.7%	9.70 (9.44)
	272	18.15	0.80	68.6%	9.96 (9.58)
	247	17.38	0.80	70.7%	9.83 (9.45)
	215	16.48	0.80	71.0%	9.36 (9.04)
	175	15.22	0.80	71.8%	8.74 (8.48)
	142	14.06	0.80	72.5%	8.15 (7.93)
	109	13.07	0.80	72.8%	7.61 (7.45)

[a] The values in parentheses stand for the average PCEs from over 15 devices.
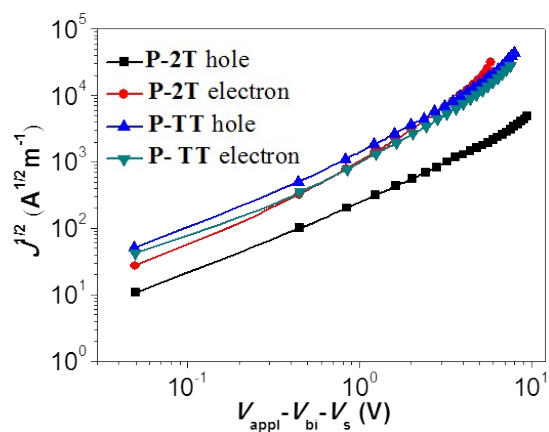
Fig. S22 Dark current density versus effective voltage characteristics of hole- and electron-only devices, with photoactive layers based on blends **P-2T**:PC$_{71}$BM and **P-TT**:PC$_{71}$BM prepared from *o*-DCB.

Table S3 Mobility results of space charge limited current (SCLC) devices based on **P-2T**:PC$_{71}$BM and **P-TT**:PC$_{71}$BM prepared from *o*-DCB.

D:A	μ_h (cm^{2}V^{-1}s^{-1})	μ_e (cm^{2}V^{-1}s^{-1})	μ_h/μ_e
P-2T : PC$_{71}$BM	1.24×10^{-3}	2.28×10^{-3}	0.54
P-TT : PC71BM	4.51×10^{-3}	3.44×10^{-3}	1.31

Table S4 2D-GIXD data of **P-2T** and **P-TT** neat and blend films.[a]

Crystallographic parameters			**P-2T** neat	**P-2T** blend	**P-TT** neat	**P-TT** blend
Out-of-plane direction	Lamellar packing (100)	q (nm^{-1})	2.38	2.48	N/A	2.49
		d-spacing (Å)	26.40	25.34	N/A	25.23
	π-π stacking (010) or (020)	q (nm^{-1})	N/A	17.78	17.40	17.60
		d-spacing (Å)	N/A	3.53	3.61	3.57
In-plane direction	Lamellar packing (100)	q (nm^{-1})	N/A	2.22	2.04	2.15
		d-spacing (Å)	N/A	28.30	30.80	29.22
	π-π stacking (010) or (020)	q (nm^{-1})	17.62	N/A	N/A	N/A
		d-spacing (Å)	3.57	N/A	N/A	N/A

[a] N/A denotes not available

References

1   X. Long, Z. Ding, C. Dou, J. Zhang, J. Liu and L. Wang, *Adv. Mater.*, 2016, **28**, 6504-6508.